Electronic Supplementary Material (ESI) for Dalton Transactions.

Supporting Information

The O-P-O bridged $Mn_2(salen)_2$ chains showing coexistence of single chain magnet and metamagnet behaviour

Ting-Ting Wang,[a] Min Ren,[a] Song-Song Bao,[a] Zhong-Sheng Cai,[a] Bin Liu,[b] Ze-Hua Zheng,[a] Zhong-Li Xu[a] and Li-Min Zheng*[a]

Table S1. Selected bond lengths (Å) and angles (°) for **1**.

Mn1-O1	1.871(2)	Mn1-O2	1.874(2)
Mn1-N1	1.979(2)	Mn1-N2	1.975(2)
Mn1-O5	2.095(2)	Mn1···O1A	3.570(2)
Mn2-O4	1.937(2)	Mn2-O3	1.890(2)
Mn2-N4	1.991(2)	Mn2-N3	1.998(2)
Mn2-O6	2.094(2)	Mn2-O4B	2.387(2)
Mn1-O1-Mn1	84.19(7)	Mn2-O4-Mn2	101.84(7)
O1-Mn1-O2	90.45(9)	O1-Mn1-N2	162.61(9)
O2-Mn1-N2	91.82(10)	O1-Mn1-N1	90.58(10)
O2-Mn1-N1	162.25(9)	N2-Mn1-N1	82.12(10)
O1-Mn1-O5	95.16(8)	O2-Mn1-O5	100.67(8)
N2-Mn1-O5	101.34(8)	N1-Mn1-O5	96.88(8)
O3-Mn2-O4	96.85(8)	O3-Mn2-N4	170.74(8)
O4-Mn2-N4	89.49(8)	O3-Mn2-N3	91.22(9)
O4-Mn2-N3	167.24(8)	N4-Mn2-N3	81.42(9)
O3-Mn2-O6	95.17(7)	O4-Mn2-O6	87.65(7)
N4-Mn2-O6	91.81(8)	N3-Mn2-O6	101.49(8)
O3-Mn2-O4B	90.87(7)	O4-Mn2-O4B	78.16(7)
N4-Mn2-O4B	83.82(7)	N3-Mn2-O4B	91.90(7)
O6-Mn2-O4B	165.16(7)		

Symmetry codes: A**:** -x, 1-y, 2-z, B**:** 1-x, -y, 2-z.

Table S2. Selected bond lengths (Å) and angles (°) for **2**.

Mn1-O1	1.875(2)	Mn1-O2	1.895(2)
Mn1-N1	1.968(2)	Mn1-N2	1.979(2)
Mn1-O5	2.082(2)	Mn1-O2A	2.532(2)
Mn2-O4	1.873(2)	Mn2-O3	1.882(2)
Mn2-N4	1.981(2)	Mn2-N3	1.985(3)
Mn2-O6	2.071(2)	Mn2-O3B	2.890(2)
Mn1-O2-Mn1A	98.36(8)	Mn2-O3-Mn2B	97.72(9)
O1-Mn1-O2	94.41(8)	O1-Mn1-N1	92.20(9)
O2-Mn1-N1	165.81(10)	O1-Mn1-N2	173.42(10)
O2-Mn1-N2	89.74(9)	N1-Mn1-N2	82.66(10)
O1-Mn1-O5	96.24(9)	O2-Mn1-O5	97.00(9)
N1-Mn1-O5	94.74(10)	N2-Mn1-O5	88.30(10)
O4-Mn2-O3	93.01(9)	O4-Mn2-N4	91.97(10)
O3-Mn2-N4	165.15(10)	O4-Mn2-N3	163.69(10)
O3-Mn2-N3	90.10(10)	N4-Mn2-N3	81.35(11)
O4-Mn2-O6	96.75(9)	O3-Mn2-O6	97.84(9)
N4-Mn2-O6	95.45(9)	N3-Mn2-O6	98.68(10)

Symmetry codes: A**:** 1-x, 1-y, -z, B**:** 1-x, 2-y, 1-z.

Table S3. Selected bond lengths (Å) and angles (°) for **3**.

Mn1-O1	1.870(2)	Mn1-O2	1.909(2)
Mn1-N1	1.974(2)	Mn1-N2	1.986(2)
Mn1-O5	2.093(2)	Mn1-O2A	2.463(2)
Mn2-O4	1.876(2)	Mn2-O3	1.885(2)
Mn2-N4	1.984(2)	Mn2-N3	1.987(2)
Mn2-O6	2.071(2)	Mn2-O3B	2.888(2)
Mn1-O2-Mn1A	98.60(8)	Mn2-O3-Mn2B	97.12(8)
O1-Mn1-O2	94.89(8)	O1-Mn1-N1	92.07(9)
O2-Mn1-N1	166.29(9)	O1-Mn1-N2	173.43(9)
O2-Mn1-N2	89.39(9)	N1-Mn1-N2	82.74(10)
O1-Mn1-O5	96.04(8)	O2-Mn1-O5	95.44(8)
N1-Mn1-O5	95.56(9)	N2-Mn1-O5	88.49(9)
O1-Mn1-O2A	90.62(7)	O2-Mn1-O2A	81.40(8)
N1-Mn1-O2A	86.73(8)	N2-Mn1-O2A	85.08(8)
O5-Mn1-O2A	172.86(7)	O4-Mn2-O3	92.69(8)
O4-Mn2-N4	92.07(9)	O3-Mn2-N4	165.53(10)
O4-Mn2-N3	163.20(9)	O3-Mn2-N3	89.97(9)
N4-Mn2-N3	81.65(10)	O4-Mn2-O6	97.74(9)
O3-Mn2-O6	99.06(9)	N4-Mn2-O6	93.83(10)
N3-Mn2-O6	98.21(9)		

Symmetry codes: A**:** 1-x, -y, -z, B**:** 1-x, 1-y, 1-z.

Table S4. The parameters obtained by fitting the ac magnetic susceptibilities for **2** under 0 Oe dc field at 2.0-3.0 K.

T(K)	χ_T / cm^3·mol^{-1}	χ_S / cm^3·mol^{-1}	ln(τ / s)	α	R[b]
2.0	2.17	2.20	-4.98	0.14	1.15×10^{-4}
2.5	6.88	2.76	-7.85	0.05	2.67×10^{-6}
3.0	5.65	2.37	-10.53	0.02	5.79×10^{-6}

Table S5. The parameters obtained by fitting the ac magnetic susceptibilities for 3 under zero dc field at 2.0-3.0 K.

T(K)	χ_T / cm^3·mol^{-1}	χ_S / cm^3·mol^{-1}	ln(τ / s)	α	R[a]
2.0	0.69	0.21	-6.16	0.11	1.58×10^{-4}
2.5	2.63	0.20	-8.67	0.03	4.02×10^{-5}
3.0	3.28	0.20	-11.13	0.01	1.72×10^{-5}

[a] $R = \sum\left[(\chi'_{obs}-\chi'_{cal})^2 + (\chi''_{obs}-\chi''_{cal})^2\right] / \sum\left[\chi'^2_{obs} + \chi''^2_{obs}\right]$

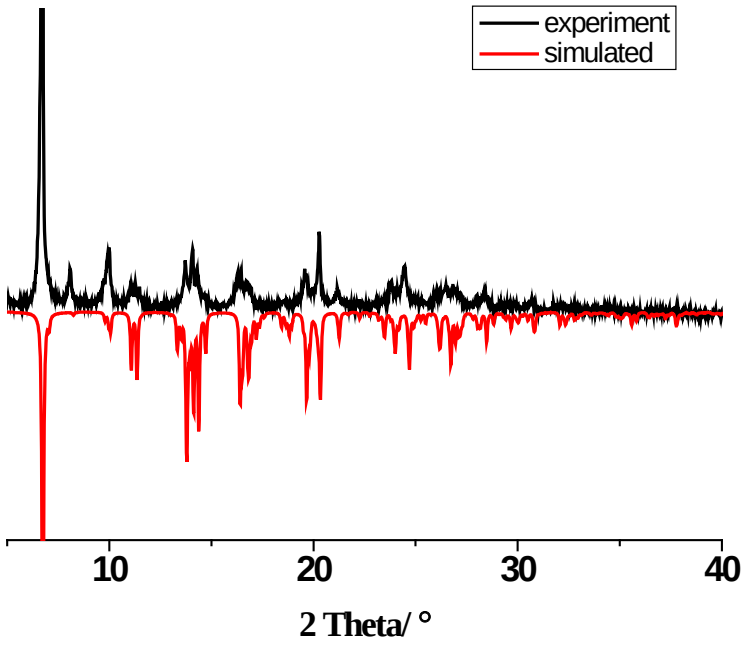

Figure S1. PXRD patterns for compound **1**.

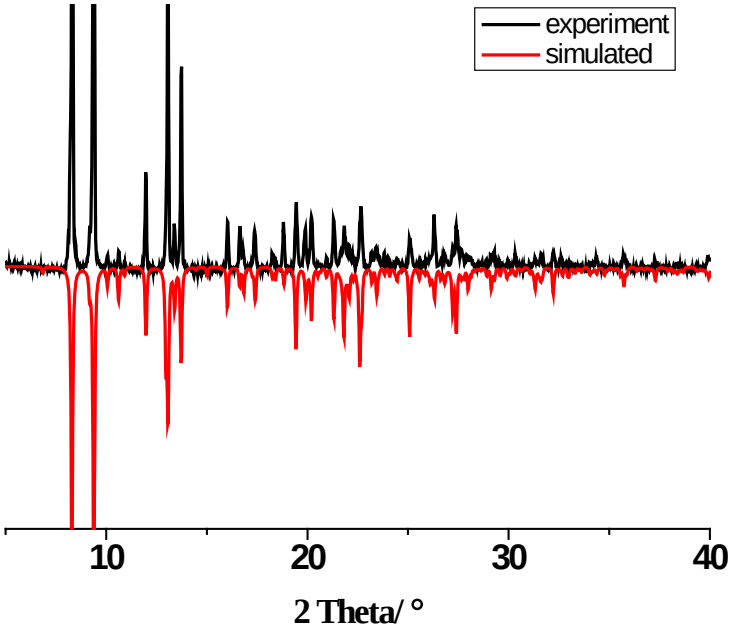

Figure S2. PXRD patterns for compound **2**.

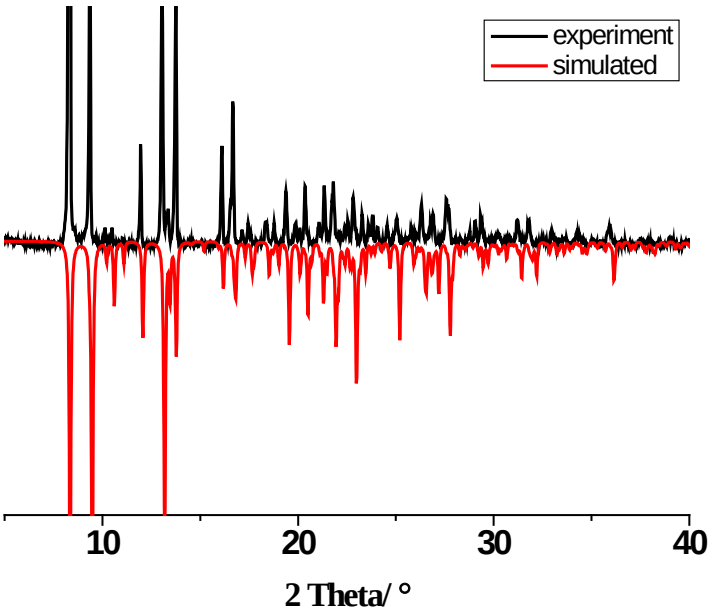

Figure S3. PXRD patterns for compound **3**.

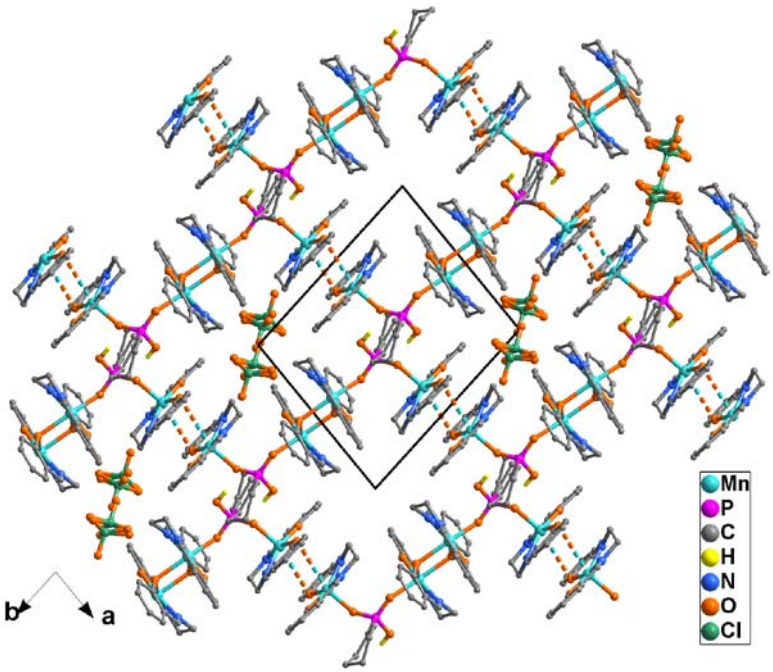

Figure S4. The packing diagram of structure **1** viewed along the *c*-axis.

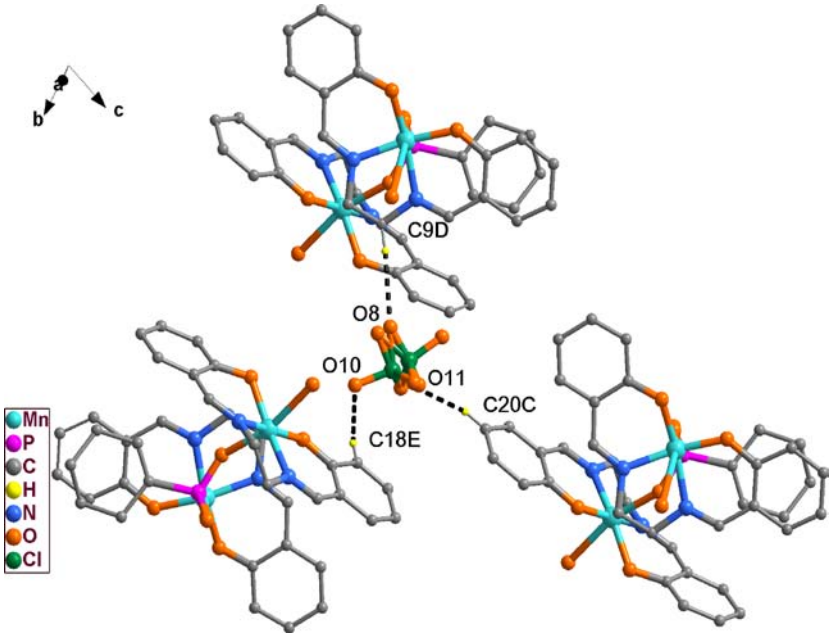

Figure S5. The hydrogen bond interactions between the ClO_4^- anion and chains in **1**. The hydrogen-bonds are shown as dotted lines. Symmetry codes: D: 1-x, 1-y, 1-z; E: 1+x, 1+y, -1+z.

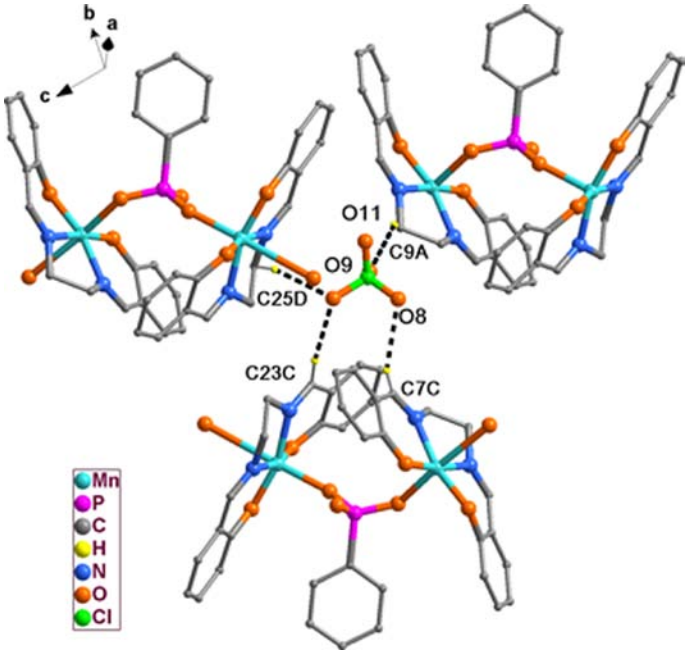

Figure S6. The hydrogen bond interactions between the ClO_4^- anion and chains in **2**. The hydrogen-bonds are shown as dotted lines. The C···O distances are 3.278(5) Å for C7C···O8, 3.207(7) Å for C9A···O11, 3.414(6) Å for C23C···O9 and 3.427(6) Å for C25D···O9. Symmetry codes: C: x, -1+y, z; D: 2-x, 1-y, 1-z.

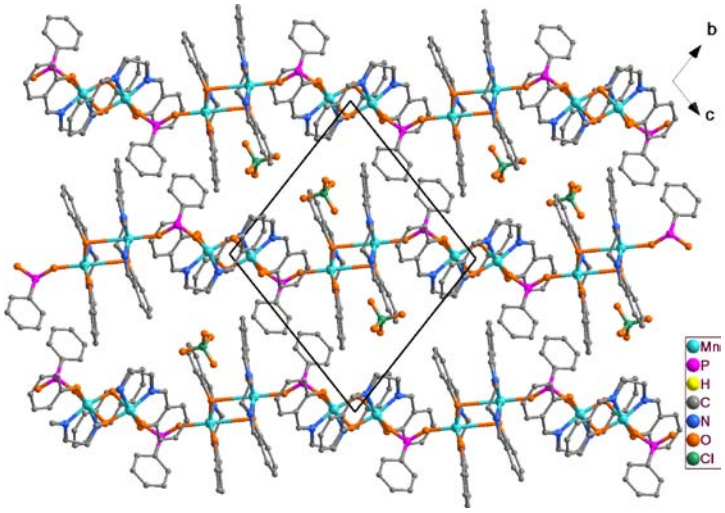

Figure S7. The packing diagram of **3** along *a* axis. All the hydrogen atoms have been omitted for clarity.

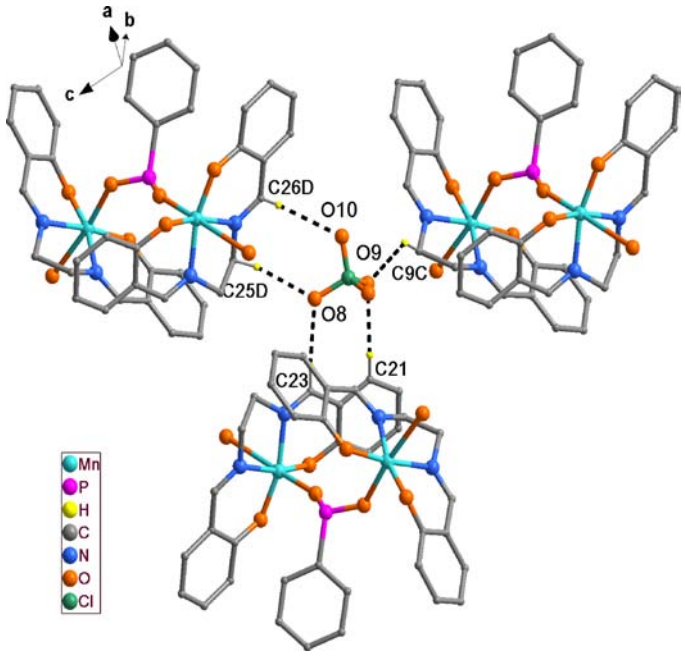

Figure S8. The hydrogen bondings among the chains around the ClO_4^- anion in **3**. Hydrogen atoms except for those are involved in the hydrogen-bondings have been omitted for clarity. The hydrogen-bonds are shown as dotted lines. The C···O distances are 3.389(5) Å for C21···O9, 3.338(4) Å for C23···O8, 3.139(5) Å for C9C···O9, 3.319(4) Å for C25D···O8 and 3.356(4) Å for C26D···O10. Symmetry code: C: 1-x, 1-y, z; D: 2-x, 1-y, 1-z.

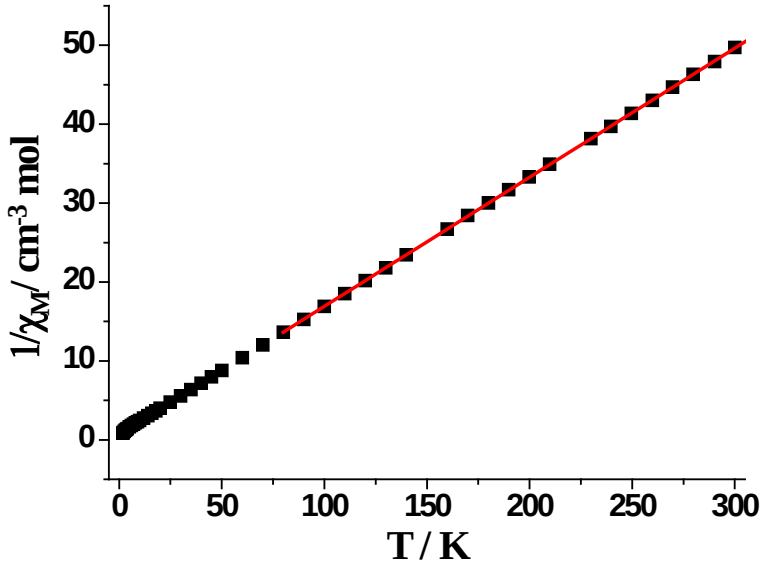

Figure S9. Plot of the $1/\chi_M$ versus T for **1**. The red solid line represents the best fit of the data above 100 K.

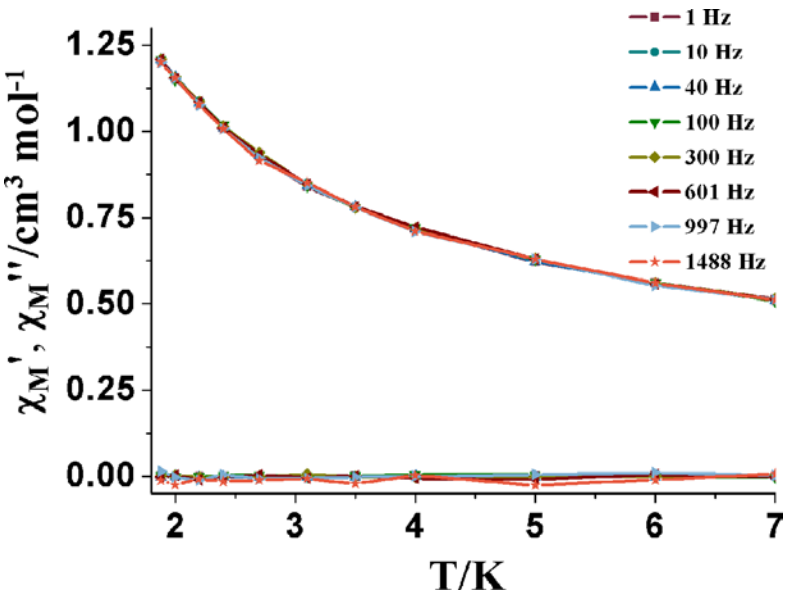

Figure S10. Plots of in-phase (χ_M', top) and out-of-phase (χ_M'', bottom) ac magnetic susceptibility versus *T* at 1, 10, 40, 100, 300, 600, 1000 and 1500 Hz for **1.**

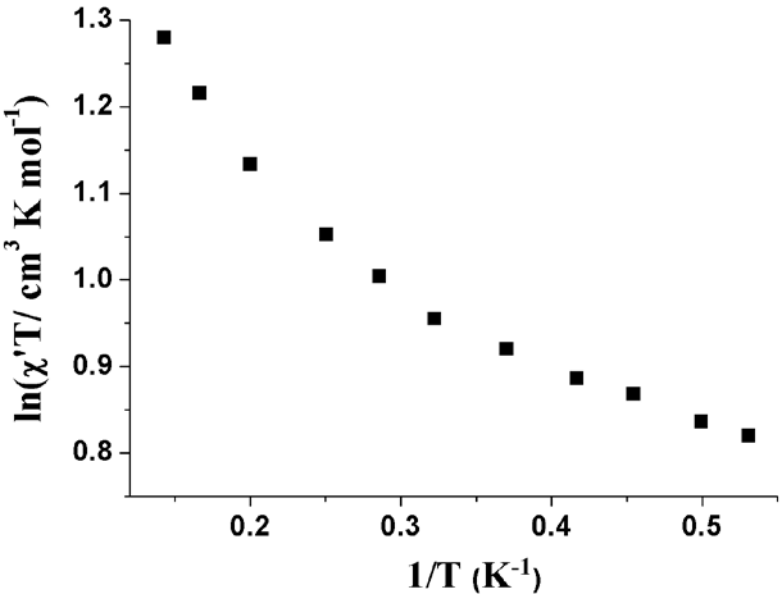

Figure S11. The ln(χ'T) versus T^{-1} plot for **1**, where χ' is equal to the in-phase ac susceptibility at 1 Hz in zero dc field.

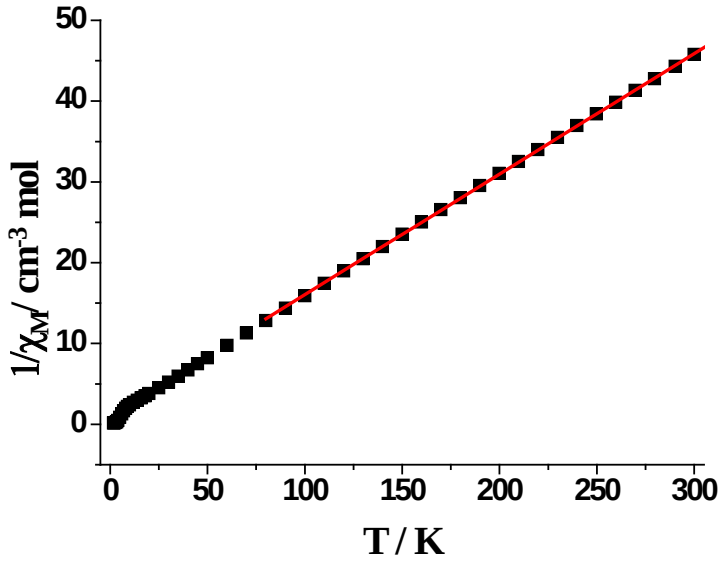

Figure S12. Plot of the $1/\chi_M$ versus T for **2**. The red solid line represents the best fit of the data above 100 K.

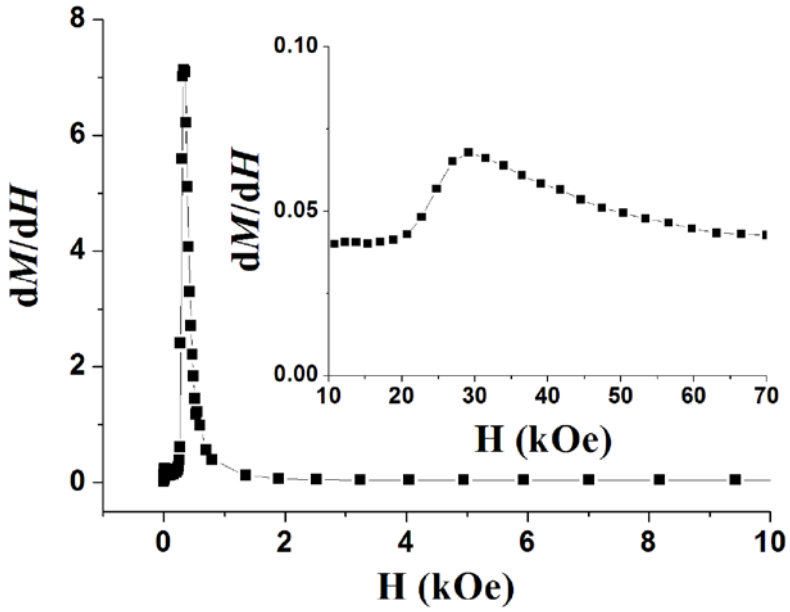

Figure S13. The derivative of field-dependent magnetization of **2** at 1.8 K.

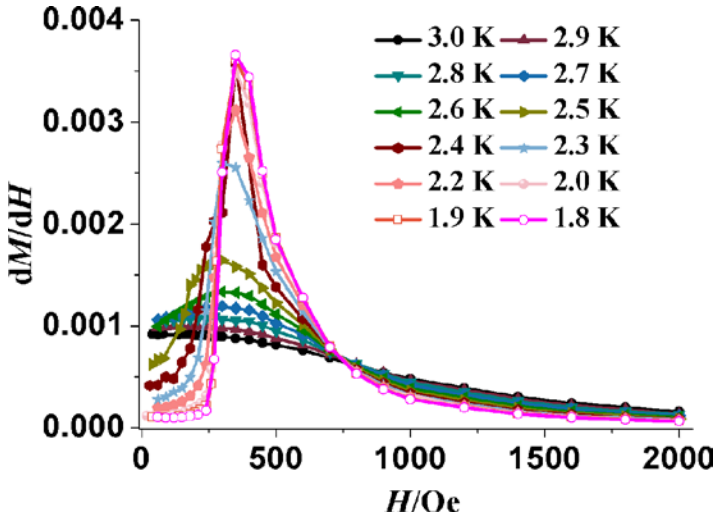

Figure S14. The derivative of field-dependent magnetization of **2** measured at different temperatures (1.8 – 3.0 K).

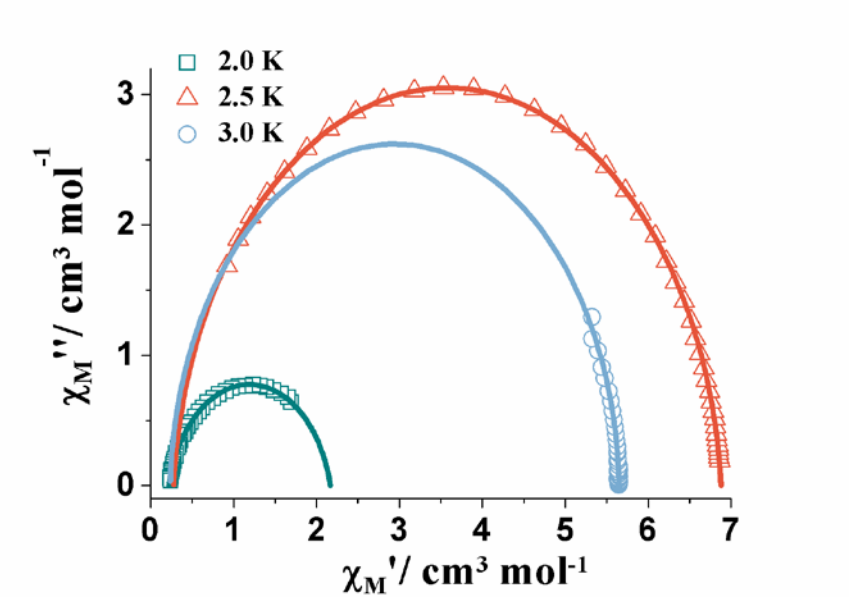

Figure S15. The Cole-Cole plots for **2** at 2.0 K, 2.5 K and 3.0 K. The open circles and the solid lines correspond to the experimental data and curves simulated using best fitting parameters, respectively.

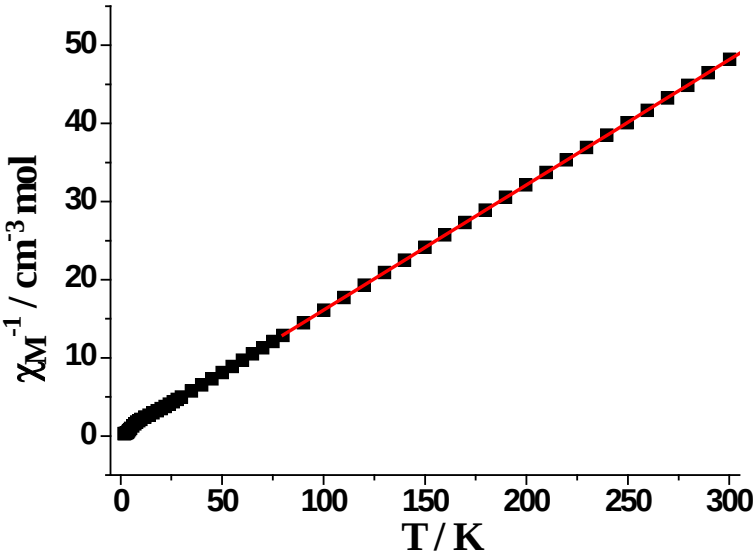

Figure S16. Plot of the $1/\chi_M$ versus T for **3**. The red solid line represents the best fit of the data above 100 K.

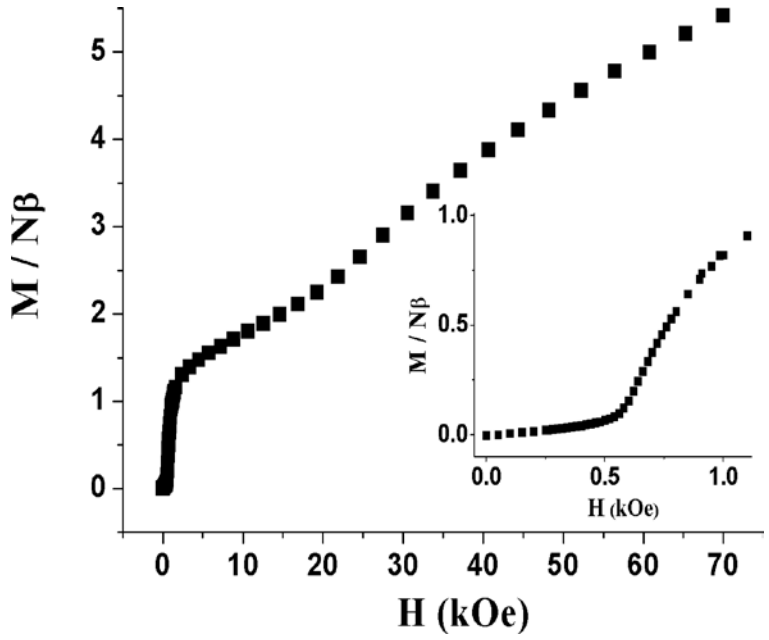

Figure S17. Field-dependent magnetization of **3** at 1.8 K. Inset shows an expansion of the low field region.

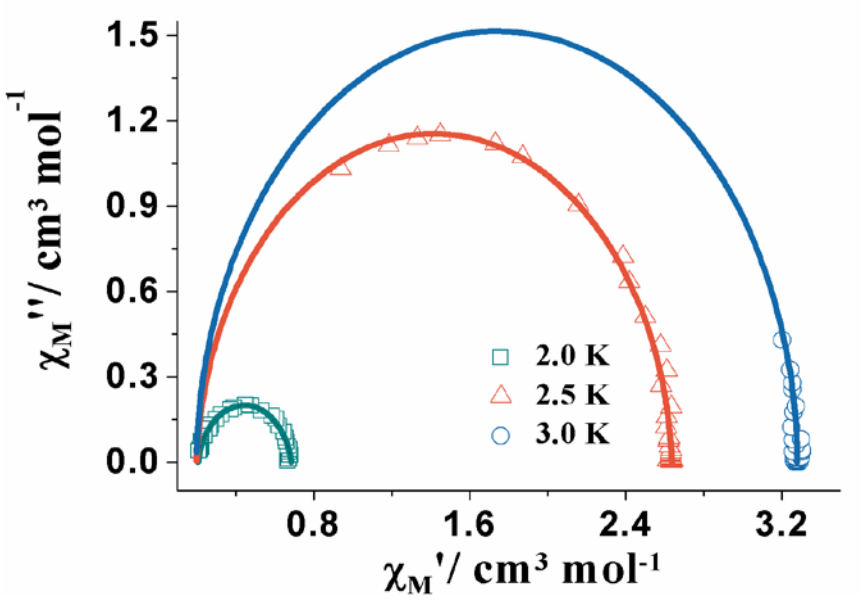

Figure S18. The Cole-Cole plots for **3** under zero dc field at 2.0 K, 2.5 K and 3.0 K. The open circles and the solid lines correspond to the experimental data and curves simulated using best fitting parameters, respectively.